BRIEFINGS IN BIOINFORMATICS. VOL 7. NO 4. 375–389
Advance Access publication November 21, 2006
doi:10.1093/bib/bbl041

Application of wavelet-based tools to study the dynamics of biological processes

Alexey N. Pavlov, Valeri A. Makarov, Erik Mosekilde and Olga V. Sosnovtseva

Submitted: 7th August 2006; Received (in revised form): 11th October 2006

Abstract

The article makes use of three different examples (sensory information processing in the rat trigeminal complex, intracellular interaction in snail neurons and multimodal dynamics in nephron autoregulation) to demonstrate how modern approaches to time-series analysis based on the wavelet-transform can provide information about the underlying complex biological processes.

Keywords: *rhythmic activity; data analysis; interaction phenomena; information processing; double-wavelet approach*

INTRODUCTION

New experimental techniques in cellular biology, physiology and other areas of biological research constantly provide us with new insights into the significance of specific biological processes. On the other hand, our understanding of the complicated interplay among these processes, and of the role of the intriguing dynamic phenomena it produces, only makes modest progress. To overcome this lack of balance between theory and experiment, first of all one requires a stronger emphasis on a systems oriented approach where mechanism-based modeling is used to establish a more complete and coherent picture. It also requires the use of concepts and methods from the rapidly growing fields of nonlinear dynamics and complex systems theory, and it requires the continuous development and improvement of tools that can help us interpret the information embedded in complex biological time series.

Contrary to the conventional concept of homeostasis, many biological control systems are unstable and operate in an oscillatory or pulsative mode. This is true, for instance, for the release of growth hormone and insulin, and in some cases the hormonal secretion becomes so erratic that one wonders whether the release patterns have significance for the regulatory function [1]. It is well-documented, though, that a rhythmic process can be more efficient in eliciting a particular response than a stable regulation.

Many cells also exhibit pulsatory variations in their membrane potentials with extremely complicated patterns of spikes and bursts. Chicken heart cells, for instance, have been shown to produce complex dynamics and synchronization phenomenon when stimulated by an external periodic signal [2]. Interacting nerve cells can also produce extremely complex and counterintuitive phenomena [3–5]. Similar forms of complexity characterize

Corresponding author. Alexey N. Pavlov, Department of Physics, Saratov State University, Astrakhanskaya Str. 83, 410026, Saratov, Russia. E-mail: pavlov@chaos.ssu.runnet.ru

Alexey N. Pavlov is an associate professor at Saratov State University (Russia) since 2002. His research interests are in dynamics of living systems and time-series analysis. He is a co-author of about 50 papers in peer-reviewed journals.

Valeri A. Makarov graduated in 1992 from the Nizhny Novgorod State University (Russia). In 1998 he got a PhD in physics and mathematics. From 1998, he has been with Complutense University of Madrid (Spain). His research interests are in nonlinear dynamics theory and its application in neuroscience.

Erik Mosekilde is a professor of physics at the Technical University of Denmark with complex systems theory and modeling of biological systems as his main interests. He is also coordinator of the EU-sponsored Network of Excellence in Biosimulation—A New Tool in Drug Development.

Olga V. Sosnovtseva is an associate professor in Biophysics at the Technical University of Denmark since 2005. Her research interests are in nonlinear dynamics and biological modeling. She is co-author of about 60 papers in peer-reviewed journals.

interactions among the intracellular regulatory processes [6], and synchronization also arises in connection with the autoregulation of nephron pressures and flows [7].

The instabilities in the regulatory processes are associated with the fact that living systems operate far from thermal equilibrium. Biologically, the complex dynamic phenomena are essential for the communication and information processing between cells, functional units and organs. Appearance of the individual rhythmic component (mode) is typically associated either with the activation of a positive feedback or with a sufficiently long delay in a negative feedback. Interactions among the modes produce a great variety of complex phenomena, including modulation of the frequency and amplitude of one mode by the presence of another, complex irregular oscillations and unusual responses to noise. The purpose of the present article is to illustrate how application of modern methods of nonlinear time series analysis can help unravel some of this complexity.

Wavelet analysis is presumably one of the most powerful tools to investigate the features of a complex signal [8–12]. The wavelet approach has shown its strength in connection with a broad range of applications such as noise reduction, information compression, images processing, synthesis of signals, etc. Like the analytical-signal approach, the wavelet transform allows one to define the instantaneous amplitude, phase and frequency for nonstationary processes.

In this article, we present an overview of some of our recent results obtained through application of wavelet analysis to the study of biological data. The article also presents a number of new results, particularly in the area of sensory information processing. The main purpose of the article is to illustrate the amount of information that one can extract from biological time series with appropriate statistical methods. In 'Wavelet analysis' we shortly review the main ideas of the wavelet analysis, and the following sections consider different applications of wavelet-based techniques. Thus, 'information processing in the trigeminal complex of the rat' is devoted to the problem of sensory information processing, where wavelets allow us to reveal a clear distinction in the response of different nerve groups to the duration of a stimulus. In 'cellular dynamics', we apply a modified wavelet technique (so-called 'double-wavelet') to analyze the interaction of different processes at the cellular level, and in 'renal autoregulation' we demonstrate the potential of the wavelet technique to study the difference between normal and pathological states in renal autoregulation. In this article we partly consider experimental data used in our recent publications. In this connection, we shall not describe the corresponding experimental procedures in details making references to previously published works.

WAVELET ANALYSIS

Traditionally, analyses of biological time series have often been performed within the framework of the following ideology: It is supposed that segments of the experimental time series are approximately stationary, and that such segments can be studied by means of statistical techniques such as, for instance, correlation measures or Fourier analysis. This approach is obviously useful if the nonstationarity is associated only with the low-frequency region of the power spectrum relative to the rhythms of interest from the physiological point of view. Such nonstationarity is treated as a slow trend and may simply be filtered out from the data [13]. However, this situation is not always true for experimental recordings. As an example, besides a slow 'floating' of the mean value, instantaneous frequencies of various rhythmic components can exhibit complex and irregular fluctuations, i.e. the nonstationarity may be associated with higher frequencies as well. Analysis of such time series using traditional statistical or spectral approaches can lead to misinterpretation of the obtained results. In particular, the coexistence of two peaks in the power spectrum of a physiological process can correspond to essentially different situations: There could be two independent modes or only a single mode whose instantaneous frequency changes in time from one value to another. Such problems serve to underline the importance of developing new, more universal tools to study the dynamics of complex systems.

From the viewpoint of possible applications, the attractiveness of a particular technique for signal processing depends on its generality, i.e. on the lack of restrictions on the signal properties. At the present, there are only few techniques that can cope with inhomogeneity and nonstationarity of biological time series. Among these, the three most well-known are: (i) the construction of an

analytical signal by means of a Hilbert transformation [14], (ii) the detrended fluctuation analysis (DFA) [15] and (iii) the wavelet analysis [8, 9].

The analytical signal approach allows us to introduce the notions of an instantaneous amplitude, phase and frequency for a random process. Thus we can analyze how these characteristics vary in time. This technique represents an effective tool for studying relations between signals, e.g. entrainment phenomena among biological rhythms.

The DFA is a tool proposed to reveal features of long-range correlations. The main idea is to interpret experimental data as 'random walk' and then analyze how this walk deviates from a local trend. Following Peng *et al.* [15], the characteristics of the DFA-method have a clear relation to the scaling exponents describing the behavior of the autocorrelation function or of the power spectrum. Thus, the DFA makes it possible to perform spectral and correlation analyses of nonstationary processes. However, for such applications, the wavelet-based multifractal analysis [16] has a number of advantages, especially for short data series. For instance, the DFA-method requires a significantly larger length of the time series and it is not as effective in the analysis of correlation properties at small time scales.

The wavelet transform of a signal $x(t)$ involves its projection onto a set of soliton-like basis functions, obtained by rescaling and translating a 'wavelet' along the time axis:

$$W(a,b) = \frac{1}{\sqrt{a}} \int_{-\infty}^{\infty} x(t) \psi^* \left(\frac{t-b}{a} \right) \mathrm{d}t, \qquad (1)$$

where ψ is the wavelet basic function and the asterisk (*) denotes complex conjugation. $W(a,b)$ is referred to as the wavelet-transform of $x(t)$, which is a function of the time scaling and the translation parameters a and b, respectively. Besides being localized in both the time and frequency domains, the basic function should possess a few additional properties, such as zero mean, boundedness and basis self-similarity (the latter means, for instance, that all wavelets constructed from a given basic function must have the same number of oscillations).

The choice of ψ depends on the purpose of the analysis. Each wavelet function has its own features in the time and frequency domains. This provides us with the opportunity to reveal specific properties of a given biological signal. The wavelet-transform is often interpreted as a 'mathematical microscope' whose optical characteristics are defined by the choice of the function ψ, and the parameters a and b determine the magnification and the focusing point, respectively. In the spectral analysis of experimental time series, one prefers complex wavelets, among which the most popular is the Morlet-wavelet whose simplified expression has the form:

$$\psi(\tau) = \pi^{\frac{-1}{4}} \exp(\, j2\pi f_0 \tau) \exp\left[-\frac{\tau^2}{2} \right]. \qquad (2)$$

The value f_0 allows us to search for a compromise between the localization of the wavelet in the time and frequency domains. The relation between time scale a and the central frequency for the function ψ is $f = f_0/a$.

Depending on the considered problem, the form of the wavelet-transform can vary: one considers either the continuous (1), or the discrete transform [10, 11]. The discrete variant involves integer translations and dilations in powers of two. This may be useful, for instance, for information compressing or in cases where it is necessary to accomplish the expansion with a minimum number of independent coefficients. In the case of signal analysis, a continuous wavelet transform (1) is usually more convenient, although this transformation possesses some ambiguity related to the continuous variation of the scaling and translation parameters. This ambiguity may actually be an advantage as it allows for a more complete analysis and a clearer presentation of the data [12].

As a result of the transform (1), the surface of coefficients $W(a,b)$ in a three-dimensional space is obtained. Visualization of this surface can be done in different ways. Often, a projection of the surface onto the plane (a, b) is considered in which tints of color mark the value of the coefficient (by analogy to geographical maps). As an alternative, the so-called 'skeleton' may be used. The skeleton consists of the lines of local extrema of the above surface. The skeleton presumably reflects the most informative features of the transform (1).

Besides the coefficients $W(a,b)$, the energy density of the signal $x(t)$ in the time scale plane can also be estimated: $E(a,b) \sim |W(a,b)|^2$. Following the definition used in [17], the coefficient of proportionality between $E(a,b)$ and $|W(a,b)|^2$ depends on both the scale and the shape of the 'mother' wavelet although in some works the simpler expression ($E(a,b) = |W(a,b)|^2$) is considered [12]. Note that the modula of the original wavelet coefficients $W(a,b)$ estimated from Equation (1) do not correspond to actual amplitudes of the rhythmic components. To study amplitude variations, it is useful to slightly

change the definition of the wavelet transform [16] or to make corrections for the energy density $E(a, b)$. In the present study, we will use the relation

$$E(a, b) = Ca^{-1}|W(a, b)|^2, \quad (3)$$

where C, a parameter that depends on the wavelet 'mother' function, is kept constant. $E(a, b)$ represents a surface in 3D space whose sections at fixed time moments correspond to the local energy spectrum. To simplify the visualization of this surface, the dynamics of only the local maxima of $E(a, b)$ or $E(f, b)$, i.e. the time evolution of the spectral peaks will be considered. In this way, all frequency components being of physiological interest can be extracted from the original wavelet transform for further analysis of their properties.

INFORMATION PROCESSING IN THE TRIGEMINAL COMPLEX OF THE RAT

Organization of the trigeminal pathway

The central nervous system (CNS) of living organisms processes enormous amount of sensory information received through the interaction with the surrounding world. The study of how this information is encoded, represented and processed in the brain is one of the most significant challenges to neurology and related sciences. Before producing sensation optical, auditive, tactile and other stimuli are encoded by their respective receptors into sequences of electrical pulses (or spikes) that are transferred to 'first' neurons in areas of the CNS (e.g. trigeminal nuclei) that perform the preprocessing of the sensory information which then passes a number of additional processing stages and finally reaches the cortex, where an internal 'image' of the external world is formed. The complexity in the representation of the sensory information increases significantly with each subsequent stage, and so does the difficulty of investigating this representation. Although the molecular and ionic mechanisms of the underlying neural activation are rather well understood [18], the properties of spike trains as information carriers remain less clear: How do these trains reflect the complexity and variety of the sensory information? How is the information transformed from one stage to the next? And how is the information from many different spike trains integrated into a coherent picture? At the moment there exist several hypotheses on the information coding in the brain with varying degrees of experimental confirmation. Sensory information can be hidden in the firing rate (frequency coding) or in the firing pattern (temporal coding) of individual neurons, or it can be populationally coded, i.e. be presented through the correlated firing of different neurons. In view of the many open questions in this field, let us examine the processing of tactile information in rats by the first relay station, the brain stem trigeminal sensory complex.

The rat perceives the majority of sensory information by means of the vibrissal pad, a highly specialized and sensitive apparatus that conveys tactile signals via the trigeminal system to the brain [19]. The length of vibrissae varies from 4–5 mm to 30–50 mm, thus providing simultaneous contact of their tips with a tangible object during whisker movements and allowing the system to cover a wide range of frequencies necessary for an effective perception of the external object.

A rat sweeps whiskers across surfaces with a frequency from 5 to 15 Hz. When a whisker touches an object, its vibration and deflection encode certain physical characteristics of the object. Specialized receptors innervated by primary afferent fibers on each whisker are excited by these movements. Figure 1 illustrates how signals from receptors (placed in vibrissae follicles) travel along the trigeminal nerve toward the brain stem where the fibers bifurcate and synapse with the 'first' neurons of the trigeminal complex [20] that contains the principalis (Pr5), interpolaris (Spi5), oralis (Spo5) and caudalis (Spc5) nuclei. The trigeminal complex performs a preprocessing of the tactile information before it is transmitted to the thalamus and then to the cortex [19]. All four nuclei are interconnected by an extensive network of internuclear fibers [21].

The purpose of this section is to demonstrate characteristic distinctions in responses to tactile stimulation of the vibrissae that exist among neurons from the three different nuclei. We propose an approach to study changes in the dynamics aiming to obtain new information concerning the neuronal response to periodic stimulation, and we show that the three groups of neurons demonstrate qualitatively different dynamics under variation of the stimulus duration.

A new approach to studying the stability of neuronal response

Characteristics of the principalis, interpolaris and oralis nuclei of the trigeminal sensory complex were

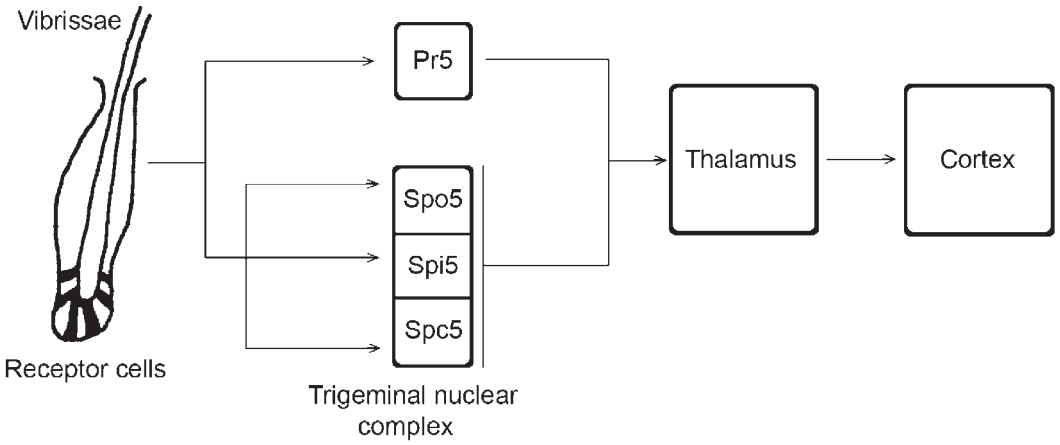

Figure 1: Main stages of the tactile information pathway: from receptor cells through the trigeminal complex via the thalamus and to the cortex.

studied under free whisker movements caused by short air puffs of 10, 50 or 100 ms durations. This type of stimulation provokes whisker oscillations closely corresponding to those observed in natural conditions. The air puffs were directed only toward one vibrissa, and signals were not recorded when other vibrissae were activated. Spontaneous spiking activity in trigeminal nuclei was extracellularly recorded *in vivo* for 180 s, and then three separated sequences of 50 stimuli of 10, 50 and 100 ms duration, respectively, at 1 Hz were applied. Further details of the experimental procedure can be found in [22]. The analyzed data set included 39 experimental recordings of single-unit activity among which: 15 recordings from the principalis, 12 from oralis and 12 from interpolaris nuclei.

A study of Pr5, Spi5 and Spo5 nuclei of the trigeminal sensory complex was reported in [22] using standard methods of data analysis (mean spiking frequency, mean response latency, per-stimulus histograms, etc.). However, these methods do not account for possible changes of neuronal activity during stimulation, and in a certain way, they are based on the hypothesis of a stereotypic response to identical stimuli. Meanwhile, deviations from this type of response are widely observed for the neurons from various parts of the brain, and accounting for such phenomena (rather than ignoring them) obviously allows us to reach a significantly better understanding of the underlying dynamical and behavioral mechanisms. In particular, Figure 2 shows an example of adaptation for a Pr5-neuron to a periodic stimulation. The activity is highest at the beginning (27 spikes/s) and after a few seconds it decreases up to about 10 spikes/s.

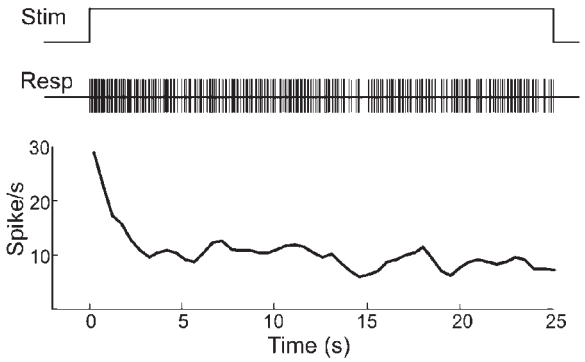

Figure 2: A representative example of adaptation of spiking activity of a neuron from Pr5 nucleus under maintained periodic stimulation of the vibrissae (10 ms air puffs at 1 Hz). (Up)—stimulus, (Middle)—neural response, (Bottom)—mean spiking rate. Note how the spiking frequency after a few seconds is reduced from 27 spikes/s to about 10 spikes/s.

If the response of a neuron to a given stimulus (short pulse) delivered to a particular vibrissa would always be the same, then periodic stimulation by a series of pulses would lead to a periodic spike train (e.g. 2 or 3 spikes/stimulus). However, in reality, we often observe aperiodic and nonstationary neural responses (Figure 2). This is the result of adaptation to external influences associated with internal processes in the neuron and with global dynamics of the neural network. A neuron typically demonstrates inhibition of the reaction to a stimulus during a certain time interval (the refraction period), or this reaction may be modified significantly depending on the time elapsed since the previous response.

As a first approach let us consider a spike train as a sequence of δ-functions (see Figure 3):

$$x(t) = \sum_i \delta(t - t_i), \tag{4}$$

where each δ-function coincides with the moment of spike generation t_i.

Using the Morlet-wavelet (2) representation of the experimental data in the form (4) allows us to analytically evaluate the wavelet-coefficients:

$$W(a, b) = \frac{\pi^{\frac{-1}{4}}}{\sqrt{a}} \sum_i \exp\left[-j2\pi f_0 \frac{t_i - b}{a}\right] \exp\left[-\frac{(t_i - t)^2}{2a^2}\right] \tag{5}$$

and to perform a complete time-frequency analysis of the spike trains, i.e. to analyze the temporal evolution of its characteristic rhythmic components. The wavelet coefficients (5) can be considered as the parameterized function $W_a(b)$, where b defines the observation time moment. It is of interest to study the neural response to a constant stimulation frequency (1 Hz in our case). If the neuron generates the same spiking pattern to all stimuli, the instantaneous frequency of the response remains constant and reflects the 1 Hz rhythm of the stimulus (Figure 4A). For an aperiodic response, however, the instantaneous frequency will show characteristic 'floatings' around the mean value. The corresponding fluctuations of the frequency will be the stronger the more significant the variations are in the neuronal response (Figure 4B).

As a numerical characterization of the stability of the response we may use:

$$S = \frac{1}{\sigma_f^2}, \tag{6}$$

where σ_f^2 is the variance of the instantaneous frequency of the neuronal activity. Note that the result of the above approach differs from that of a simple statistical analysis such as the construction of per-stimulus histograms. Such histograms will be very similar, for instance, for the two spike trains shown in Figure 5, while the parameter S will reveal essential distinctions because it accounts for the dynamical changes. A stereotypical neuronal response of any complexity will attain a constant value of f (Figure 4A) and, consequently, produce an infinite value of the stability S. Rather than emphasizing the structure of the spike pattern the stability measure accentuates the spike to spike differences in the response. Thus, we have a parameter that allows us to quantify the long-term nonstationarity in the neural response. Note that this measure is also different from the sliding window averaging shown in Figure 2.

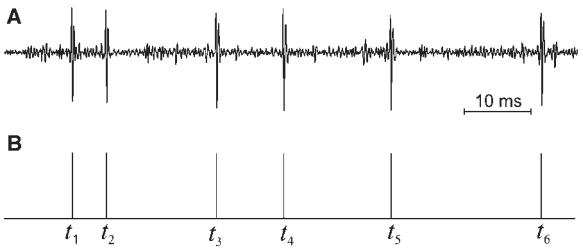

Figure 3: Representation of a spike train in the form of a series of δ-functions. (A) Band-pass filtered extracellular spikes recorded in Pr5 nucleus. (B) Each spike is associated with a δ-function.

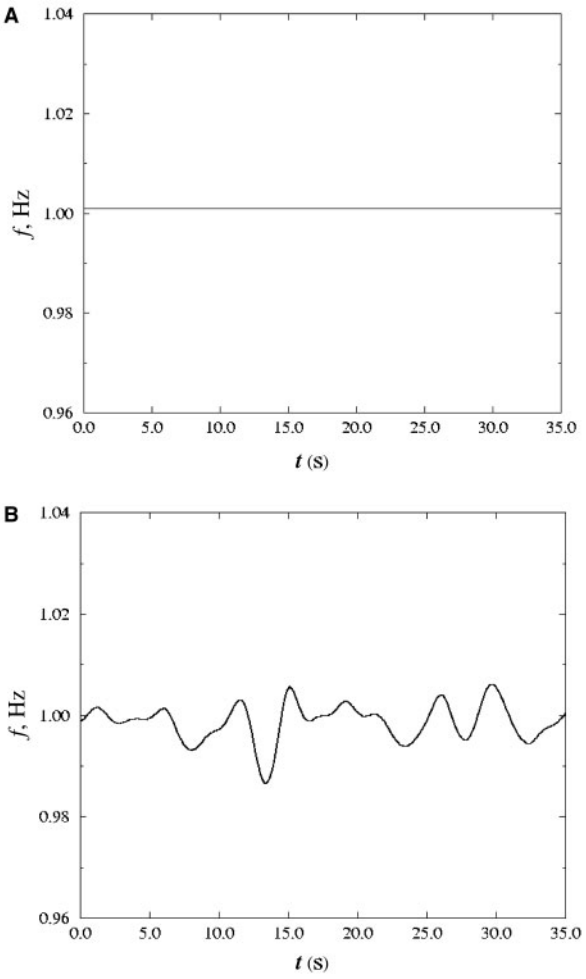

Figure 4: Dynamics of the instantaneous frequency for a periodic (A) and an aperiodic (B) neuronal responses to a l Hz stimulation. Note that the modulation observed in (B) never reaches a steady state value.

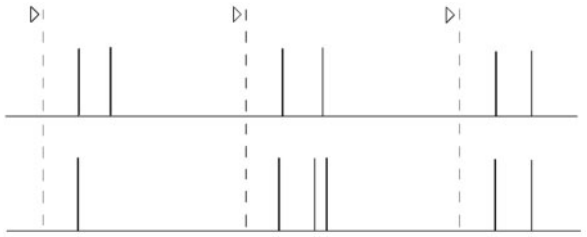

Figure 5: Examples of different neuronal response to the same stimulation. The per-stimulus histograms will be fairly similar in both cases, whereas the stability parameter S defined in (6) will reveal clear distinctions. Dashed lines mark the moments of stimulus onsets.

By estimating the response stability of a series of experimental recordings, we have been able to reveal differences in the neuronal reaction to variation of the stimulus duration between principalis, interpolaris and oralis nuclei. We have first calculated the parameter S for the three types of neurons (from three different nuclei) and the three types of stimulation (10, 50 or 100 ms). We have thereafter determined the stimulus duration that leads to the highest stability in the response for each type of neuron (i.e. to the minimal deviations from the stereotypic response during the whole stimulation)—Figure 6A. With a view of quantifying the changes of this stability when the stimulus duration increases ($10 \rightarrow 50 \rightarrow 100$ ms), we have determined the number of neurons satisfying the conditions: $S_{50} > S_{10}$ and $S_{50} > S_{100}$, where the subscript denotes the considered pulse duration (Figure 6B).

In the case of Pr5-neurons, the stability parameter S takes its maximal value for the intermediate duration of the stimuli (50 ms). This is observed for ~53% of cells. For 73% of Pr5-neurons, the response to 50 ms stimulation is more stable than to air puffs of 100 ms duration. Quite similar dynamics is observed for Spi5 neurons: 67% of the cells show a most stable response at 50 ms stimulation, and only a single cell demonstrates the presence of maximal stability at 10 ms stimulation. The value of S increases at the transition $10 \rightarrow 50$ ms for ~92% of cells. Thus, Pr5- and Spi5-neurons are characterized by rather similar types of reaction to variation of stimulus duration from the viewpoint of trial to trial stability. The most prominent difference in their responses is observed for the shortest (10 ms) stimulus duration, when about twice more neurons from Pr5 show better stability. Spo5-neurons demonstrate

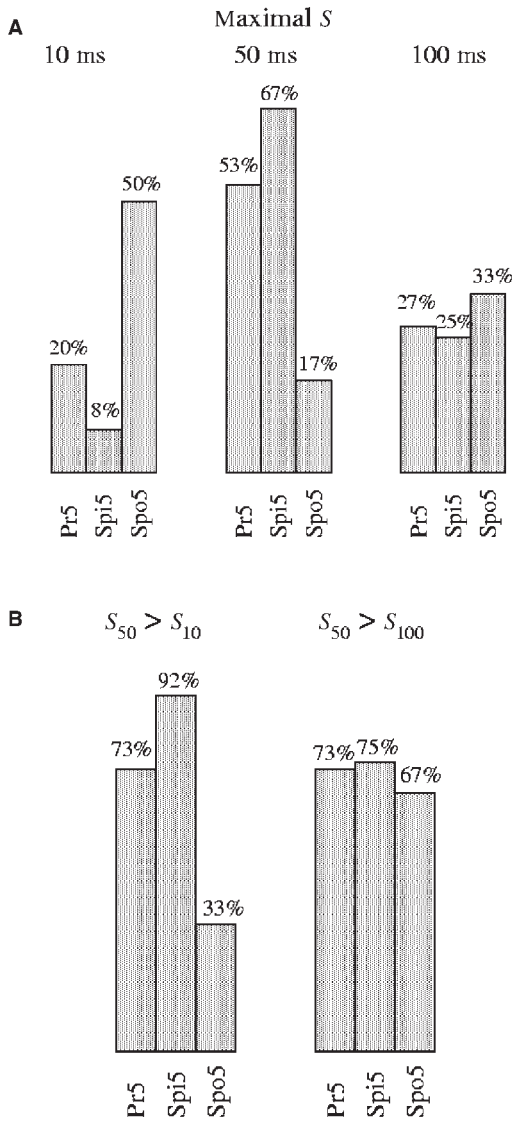

Figure 6: Comparative analysis of the spiking pattern stability of the response of Pr5, Spi5 and Spo5-neurons under 1 Hz stimulation of vibrissa by pulses of air puffs of different durations. (A) Percentage of the neurons showing maximal stability S for the corresponding stimulus duration. (B) Percentage of the neuron showing an increase of the response stability for the intermediate stimulus duration (50 ms).

completely different type of response. Maximal stability at 50 ms stimulation was observed for only 17% of these cells. Most of the neurons (~50%) reached the maximally stable response for the shortest 10 ms stimulation and only for 33% of the cells the value of S grew up with the increase of the stimulus duration from 10 to 50 ms.

This analysis allows us to make conclusions about the different response dynamics of neurons from the three nuclei: Whereas the stability of the

Spo5-neurons has a minimum at the intermediate stimulus duration ($S_{10} > S_{50} < S_{100}$), Pr5- and Spi5-neurons show the opposite behavior, they reach the most stable response at the intermediate value ($S_{10} < S_{50} > S_{100}$). Hence, we can suppose that there is an optimal stimulus duration that provides stable firing of neurons from the Pr5- and Spi5-nuclei and at the same time Spo5-neurons show the most significant variability. This may mean that principalis and interpolaris nuclei process the tactile information in a similar way, paying attention mostly to the fast and precise identification of the presence of tactile stimuli, while the oralis nucleus works on a longer time scale processing the fine structure of the stimulus. Thus, our novel method allows getting a new interpretation of the tactile information processing in the trigeminal complex of the rat. In contrast to the traditional electrophysiological approach (a study of neuronal response averaged over trials), the proposed stability measure reveals essential differences in the time evolution of the responses of Pr5, Spi5 and Spo5-neurons mostly localized in the range of short (10 ms) to intermediate (50 ms) stimulus durations.

CELLULAR DYNAMICS

Study of intracellular processes with interference microscopy

Cell dynamics involves a number of regulatory processes that occur over many different time scales both in the plasma membrane and in the various cytoplasmic compartments. A study of nonlinear interaction phenomena between these processes allows us to establish a better understanding of cellular regulation and function. Standard experimental approaches (patch clamping, intracellular registration of membrane potentials and fluorescent microscopy) only allow us to analyze the processes individually. Moreover, these tools may distort the cellular processes or damage neuron structures.

An extremely promising approach to studying cooperative phenomena in intracellular dynamics is based on the use of interference microscopy [23]. With this technique one measures the optical path difference between a laser beam transmitted through the object (e.g. a biological cell) and reflected from a bottom mirror and a reference beam reflected from the control mirror [23]. The phase height relief reflects the location of various organelles and plasma membrane structures. The relief changes in time, and these variations provide information on the dynamics of the local refractive index resulting from processes in the plasma membrane and inside the cell, e.g. changes in membrane bound proteins, variations in the local Ca^{2+} concentrations, or motion of vesicles carrying neurotransmittors to the cell surface.

Experiments were performed on isolated pond snail (*Lymnaea stagnalis*) neurons. Details of these experiments are described in our recent article [6].

Interaction among intracellular processes

Unraveling the complexity of information contained in interference-microscopic time series obviously poses some difficulties with respect to identifying the processes that are responsible for the various signal components. Some of these difficulties can be addressed by measuring at different positions in the cell. One can also change the external conditions (e.g. the salinity of the surrounding solution) and add chemical components that influence the cellular processes (e.g. by blocking certain ion channels). However, by revealing the mutual interactions among the signal components, a sufficiently skillful time series analysis can also provide important insights.

Interaction phenomena between the coexisting modes in the dynamics of a biological system are reflected in the temporal evolution of the instantaneous frequencies and amplitudes of the existing rhythms. In particular, the mode-to-mode interaction may reveal itself in the form of a modulation where the instantaneous amplitude or frequency of one (faster) mode is modulated by the presence of another (slower) mode. Aiming to study modulation properties, we propose to use the following approach. The time dependence of the instantaneous frequency is considered as input signal for a second wavelet-transform (1) [25, 26]. Again, the wavelet coefficients and the energy density are estimated and the simplified visualization of the energy density is considered. The latter will contain information about all modes involved in the modulation process. In the case of nonstationary dynamics we can examine how the features (characteristics) of the frequency modulation are changed in time. By analogy, instead of the instantaneous frequency of the fast dynamics we can take the instantaneous amplitude of this mode and, thus, study the properties of amplitude modulation of the fast rhythm.

This approach, which we shall refer to as a *double-wavelet analysis* [27, 28] allows us to characterize

the nonstationary temporal dynamics of a modulated signal, i.e. to detect all components that are involved in the modulation, estimate their contributions and analyze whether the modulation properties change during the observation time.

Figure 7A illustrates an example of the power spectrum estimated for the refractive index recordings in the low-frequency range. Inspection of this figure clearly shows the presence of several rhythmic components with frequencies around 0.1, 0.2–0.4, 1 and 3 Hz. Aiming at a better understanding of cellular dynamics, we have tried to associate each rhythm with a particular process in the cell [6]. We suppose that the frequency range shown in Figure 7A represents processes in the plasma membrane. In particular, slow processes with the frequencies around 0.1 Hz probably originate from reorganizations in the plasma membrane such as lipid rafts and protein movements, changes of the amount of membrane-bound ions and, related hereto, local fluctuations of the membrane fluidity and transmembrane potential [29–31]. Rhythmic components in the next frequency range (0.2–0.4 Hz) are considered to be associated with the dynamics of Cd^{2+} ions (a blocker for Ca^{2+} channels) [32]. According to Schutt *et al.* [33], neurons in the ganglia of mollusca *Helix aspersa* possess an intrinsic 1 Hz activity and a nonspecific induced activity at 1.5 and 3 Hz. Moreover, Peixoto *et al.* [34] found that during the first 3 h after isolation, *Helix* neurons show a spontaneous rhythmic activity with 1–10 Hz frequencies. Hence, the prominent spectral peaks with frequencies around 1 and 3 Hz may correspond to subthreshold changes of the membrane potential and/or to spontaneous rhythmic activity.

The coexistence of rhythmic components in the nonlinear biological system leads to their mutual interaction. As we can see from Figure 7B, instantaneous frequencies of faster rhythmic components (around 1 and 3 Hz) oscillate in time. These variations are likely to arise from frequency modulation by the slower intracellular processes. The instantaneous frequencies of the rhythms between 0.1 and 0.4 Hz demonstrate relatively constant values during the observation time (this may, obviously, be connected with the relatively short duration of the available experimental recordings). The 1.3 Hz mode, however, shows a modulation with two full cycles during the 20 s observation time. This corresponds to the

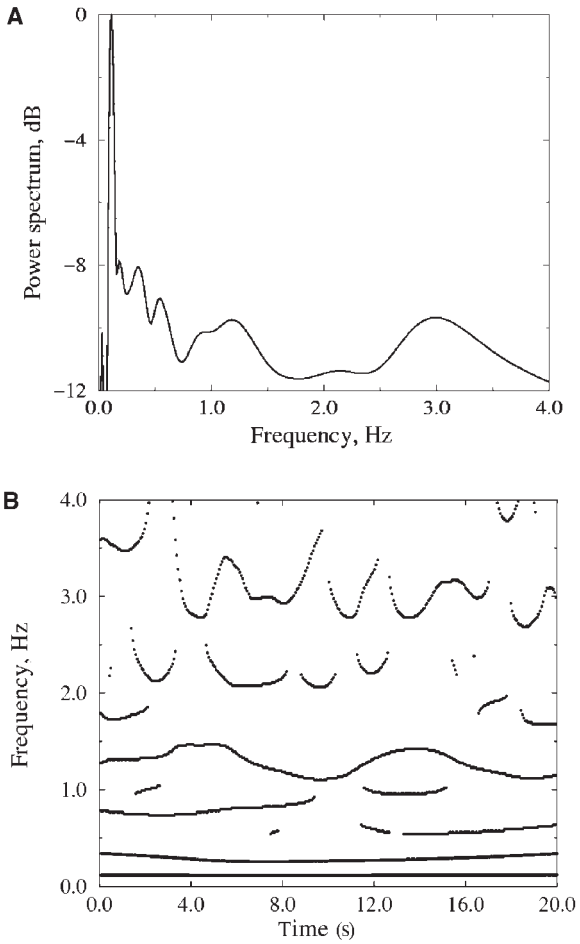

Figure 7: (A) Power spectrum calculated via the wavelet technique. (B) The dynamics of all local maxima of the energy density reveals variations of the rhythmic behavior with time. In particular we note how the 1.3 Hz mode is modulated by a 0.1 Hz signal.

frequency of the 1.3 Hz mode being modulated by the presence of the 0.1 Hz mode. The obvious conclusion is that these two modes are associated with strongly interacting processes. Similarly, the frequency of the 3–4 Hz mode performs 7–8 oscillations during the 20 s observation period. This corresponds to the modulation of this frequency by the 0.3–0.4 Hz mode. A more detailed analysis of the nonlinear interactions between the coexisting oscillatory modes can provide quantitative information about the degree of interaction between different mechanisms in the cell functioning.

Our analysis was based on about 200 recordings. Besides the instantaneous frequencies, we have also analyzed the instantaneous amplitudes of the low-frequency modes (i.e. below 5 Hz). Further, we have quantified the intensity of mode-to-mode

interactions in terms of the modulation depth separately for the amplitude and for the frequency modulation [6]. Figure 8 shows that the rhythmic components at 1 Hz (black circles) and 2–4 Hz (white circles) are clearly separated with respect to modulation depth in the case of frequency modulation (Figure 8A) and with respect to modulation frequency in the case of amplitude modulation (Figure 8B). We consider this to imply that different biological mechanisms are involved in the regulation of the 1 Hz and the 2–4 Hz rhythmic activities.

The above results clearly reveal the presence of nonlinear interactions among the cellular processes in the form of frequency and amplitude modulation of the fast processes by the slower processes. Further analyses of refractive index dynamics and the relations between the observed frequencies of the refractive index changes are presently underway. Such analyses are expected to provide a more detailed physiological understanding of the interaction of cellular processes on different time-scale, in different neuron compartments and at rest conditions as well as under the influence of external stimuli.

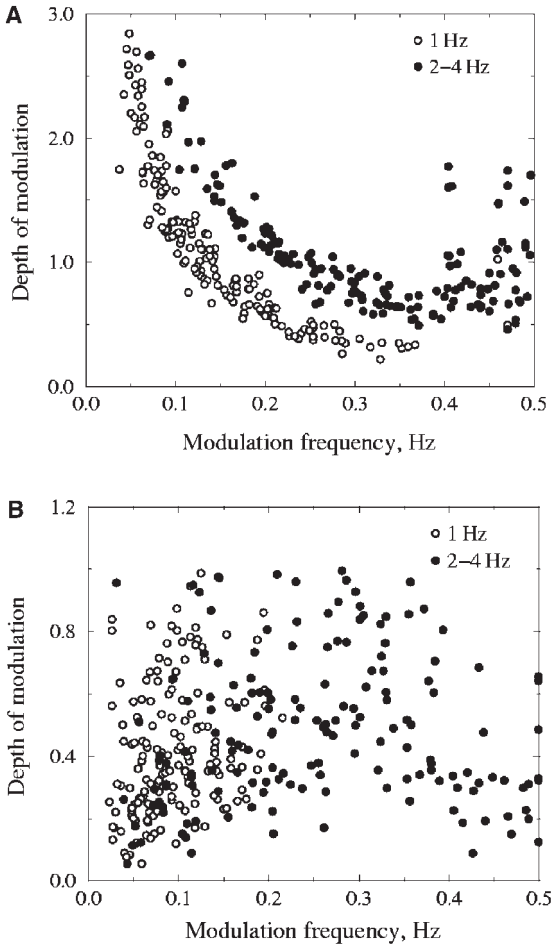

Figure 8: Distribution of modulation depths with the modulation frequency as a parameter for the 1 Hz and 2–4 Hz rhythmic components in the cases of (A) frequency and (B) amplitude modulation.

RENAL AUTOREGULATION

Multimode dynamics in nephron autoregulation

In this section, we shall consider application of time series analysis to study nonlinear interactions between two mechanisms of renal autoregulation. It is well known that the kidneys play an important role in regulating the blood pressure and maintaining a proper environment for the cells of the body. The measurements to be reported in this section were performed in rats. A rat kidney contains ~30 000 nephrons as compared with the 1 million nephrons in a human kidney. The process of urine formation starts with the filtration of plasma in the glomerulus, a system of 20–40 capillary loops. The presence of a relatively high hydrostatic pressure in this system allows water, salts and small molecules to pass out through the capillary wall and into the proximal tubule. Blood cells and proteins are retained, and the filtration process saturates when the protein osmotic pressure balances the hydrostatic pressure difference between the blood and the filtrate in the tubule. For superficial nephrons, the proximal tubule is visible in the surface of the kidney and easily accessible for pressure measurements.

To protect its function against variations in the arterial blood pressure, the individual functional unit of the kidney (the nephron) possesses a feedback mechanism (the so-called tubuloglomerular feedback) that regulates the incoming blood flow depending on the NaCl concentration of the fluid that leaves the loop of Henle. As experiments on rats have shown [35–37], this feedback regulation can become unstable and generate self-sustained oscillations in the proximal intratubular pressure with a typical period of 30–40 s. With different amplitudes and phases the same oscillations are manifest in the distal intratubular pressure and in the chloride concentration near the terminal part of the loop of Henle. The observed oscillations are fairly regular for normotensive rats and highly

irregular for so-called spontaneously hypertensive rats, i.e. rats that are genetically disposed for high blood pressures [35].

Another rhythmic component in the nephron autoregulation that can be revealed by wavelet analysis [38] is associated with a myogenic mechanism representing the intrinsic response of the smooth muscle cells in the vascular wall to changes in the TGF-signal as well as to other stimuli. This mechanism operates at 0.1–0.25 Hz. An increase of the transmural pressure elicits a contraction of the vascular smooth muscle causing a vasoconstriction and an increase in the resistance of the afferent arteriole. Since both the above mechanisms act on the afferent arteriole to control its hemodynamic resistance, the activation of one of the mechanisms modifies the response of the other. Interaction between these mechanisms can lead to various modes of intranephron synchronization [39]. Interaction between the two modes can also lead to modulation of the faster mode by the slower dynamics [27, 28]. Let us consider some of the features of this modulation.

Figure 9 displays an experimental recording of the proximal tubular pressure in surface nephrons in a rat together with the temporal behavior of the instantaneous frequencies associated with the slow (f_{slow}) and the fast (f_{fast}) oscillatory modes in the dynamics of the nephron. We can clearly see that both modes are well expressed. The first of them (f_{slow}) remains practically constant while the second (f_{fast}) changes in time. Moreover, since Figure 9B represents the values of the instantaneous frequencies, some value of the energy density is associated with each point as shown in this figure. This means that we can extract not only the time dependences of the instantaneous frequencies but also the dependences of the instantaneous values of the energy densities (or the instantaneous amplitudes).

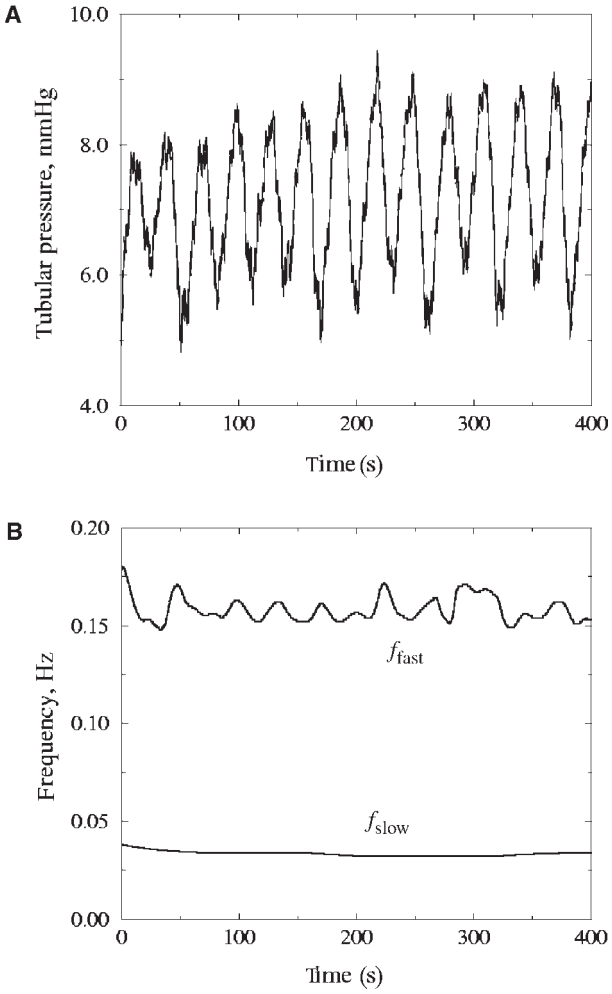

Figure 9: Experimental recording of the proximal tubular pressure in a cortical nephron of a rat kidney (A) and the extracted frequencies of rhythmic components. The search for f_{slow} and f_{fast} was performed in the ranges [0.02–0.07] Hz and [0.1–0.25] Hz, respectively. The frequency step in the wavelet transform was chosen to be 0.001 Hz.

Mode-to-mode interaction in individual nephron

The extracted time dependences of the instantaneous frequencies and amplitudes can further be analyzed to extract information about the modulating frequency and the depth of modulation. In particular, we can study the frequency and amplitude modulations of the myogenic mode by applying a second wavelet-transformation to the temporal variations in the instantaneous frequency or amplitude of this mode. As shown in Figure 10, the modulation depth can show essential variations demonstrating that the strength of the mode-to-mode interaction does not remain constant. Moreover, we have found that the numerical values of the depth of the frequency modulation (M_f) are significantly different for a normotensive ($M_f \approx 0.35$ in the average) and a hypertensive rat ($M_f \approx 1.1$ and strongly varying). Here, $M_f = \Delta\omega/\Omega$, where $\Delta\omega = (\omega_{max} - \omega_{min})/2$ and Ω is the modulation frequency. For nonstationary processes, $\Omega(t)$ is determined via a single-wavelet technique while the peak to peak frequency variation $\Delta\omega(t)$ is determined via the double-wavelet technique.

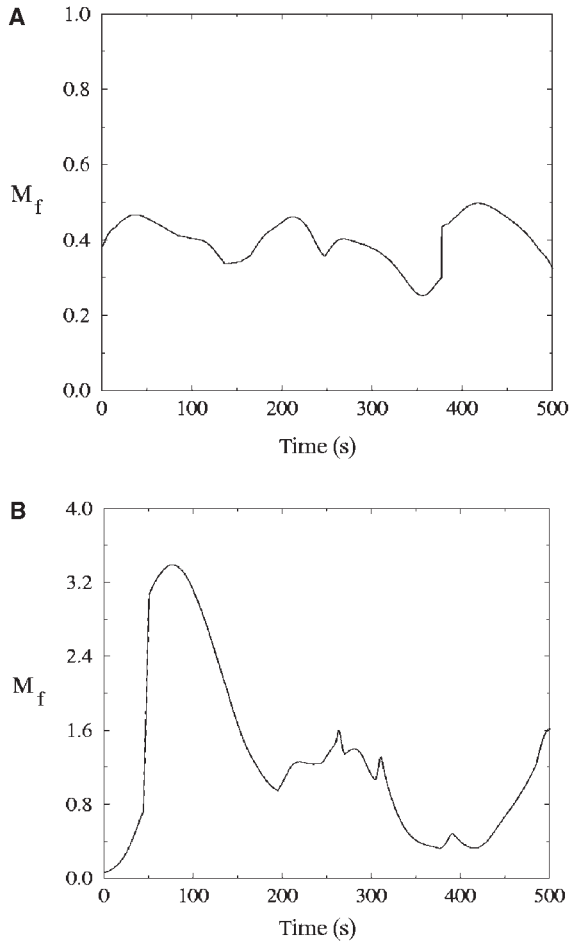

Figure 10: Temporal variations in the depths of frequency modulation for a normotensive (A) and a hypertensive (B) rat. The frequency modulation depth M_f measures how much the frequency of the fast (myogenic) mode is modulated by the slower (tubuloglomerular) mode.

Analogous studies can be performed for the instantaneous amplitudes of the fast mode. In this way, we obtained the values $M_a \approx 0.33$ and $M_a \approx 0.55$ for the depths of the amplitude modulation in the normotensive and the hypertensive rat, respectively. We conclude that the amplitude modulation is less expressed than the frequency modulation. This observation may provide an important testing criterion for alternative models of the interaction between the two modes.

We have performed a statistical survey of these results for a series of experiments. We used 76 recordings, among which 34 were from normotensive and 42 from hypertensive rats. Animal preparation and the experimental procedure are described in the literature [35–37]. Figure 11 illustrates

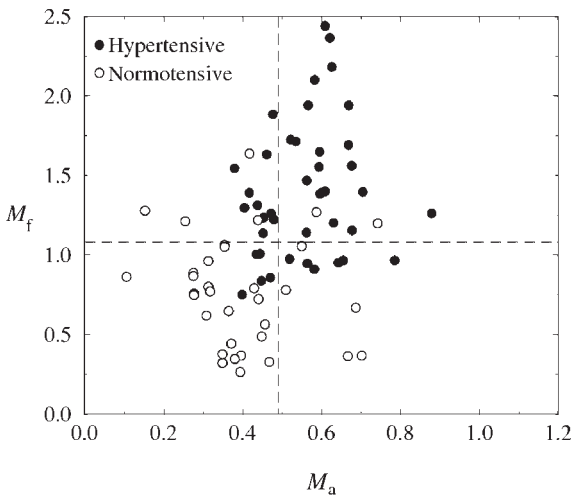

Figure 11: Distribution of depths of frequency and amplitude modulation of the myogenic mode by the TGF-mediated mode.

the distribution of depths of frequency and amplitude modulation for hypertensive (black circles) and normotensive (white circles) rats. Inspection of the figure clearly shows that there is a well-defined distinction between the two rat strains for both the amplitude and the frequency modulation, although the latter effect is more clearly expressed. Over the complete data set, the mean values of the modulation depth with standard error of the mean are $M_a = 0.49 \pm 0.02$ and $M_f = 1.08 \pm 0.06$ as indicated by the dashed lines in Figure 11. It is clearly seen that the depth of modulation and, hence, the nonlinear interaction between the involved mechanisms are stronger for hypertensive than for normotensive rats. The mean values are $M_a = 0.40 \pm 0.02$ and $M_f = 0.74 \pm 0.06$ for normotensive rats, while $M_a = 0.55 \pm 0.02$ and $M_f = 1.35 \pm 0.06$ for hypertensive rats. The number of nephrons with a frequency modulation that exceeds the average value is higher for hypertensive rats (75%) than for normotensive rats (18%). For the amplitude variations, we obtained 64% and 21%, respectively.

Very low frequency components of unknown origin also participate in the mode-to-mode interaction and influence the above two mechanisms of renal autoregulation. Thus, the modulation spectrum for the TGF-mode (Figure 12A) contains a sharp peak at a frequency of about 0.006 Hz, and the modulation spectrum for the myogenic mode (Figure 12B), besides the peak at about 0.03 Hz reflecting the TGF-dynamics, also contains a clear peak at a frequency of about 0.006 Hz.

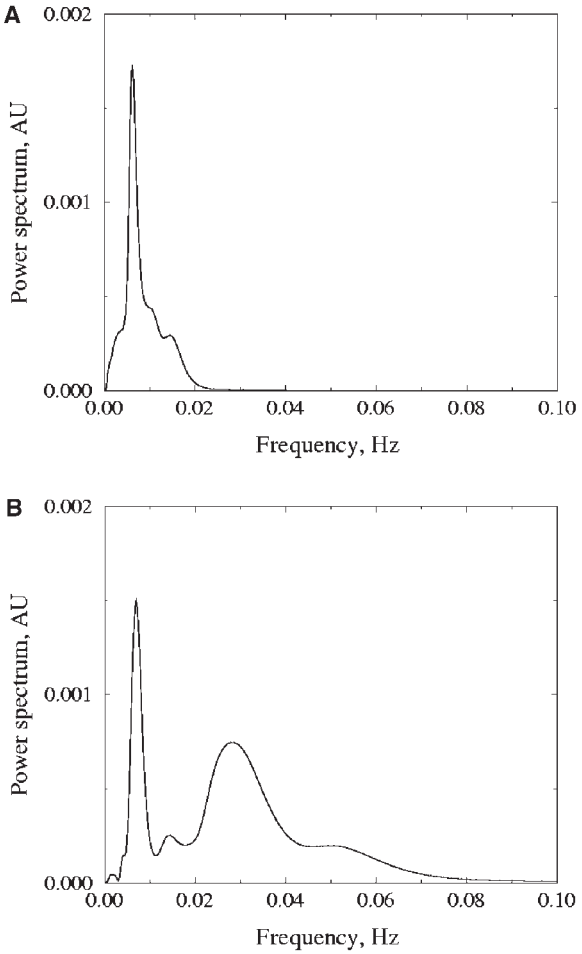

Figure 12: Power spectra of amplitude modulation for TGF (A) and for myogenic (B) dynamics for a nephron from a hypertensive rat. Note the peaks occurring at very slow dynamics.

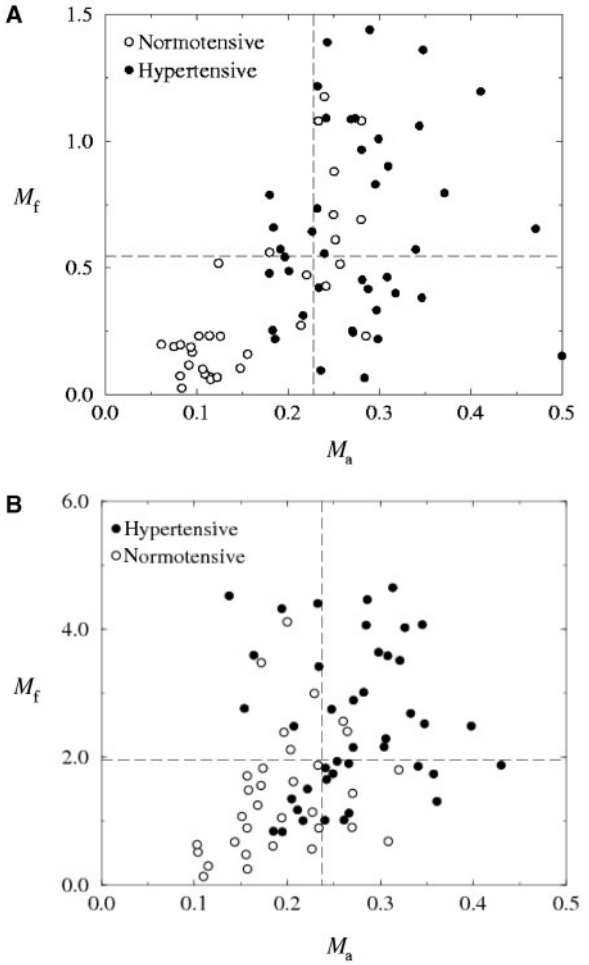

Figure 13: Distributions of depths of frequency and amplitude modulation of the TGF-mode (A) and the myogenic mode (B) by very slow oscillations.

Figure 13A and B shows distributions of frequency and amplitude modulation depths for the TGF-mediated mode (Figure 13A) and the myogenic mode (Figure 13B) as caused by the very slow dynamics. Again, the spontaneously hypertensive rats demonstrate a higher depth of modulation and, therefore, a stronger mode-to-mode interaction. The revealed phenomena and, in particular, the role of very slow dynamics in the renal autoregulation need further physiological interpretation.

Based on the above results, we suggest that the mechanism of regulation of the afferent arterial blood flow is more complex than previously assumed. In hypertension, the active parts of the blood vessels demonstrate increased variability in their oscillations, i.e. regulation of the flow is associated not only with changes in vascular diameters but also with an accompanying adjustment of the frequency of the vascular oscillations.

We would like to note that amplitude modulation of the myogenic dynamics by the tubuloglomerular mechanism has previously been demonstrated [40], but frequency modulation has never been observed in the renal circulation, or in other vascular beds. From a physiological point of view, we can associate the strong variations in M_f observed particularly for the hypertensive rats with nonlinear effects in the activation of the smooth muscle cells in the arteriolar wall. At low activation level, these cells operate in a relatively incoherent manner. With increasing activation, however, the cells start to perform self-sustained and synchronized oscillations with a period that depends on the activation level.

CONCLUSIONS

In the course of the last years, wavelet-based methods have found many different applications in the analysis of biological systems. The appearance of this tool has essentially extended our ability to extract information from experimental research. Living systems typically demonstrate complex irregular behaviors whose characteristics continuously change in time. Application of standard methods of statistical analysis in such situations is based on the *a-priori* assumption that we deal with stationary processes. However, it is very difficult (or even impossible) to support this assumption, especially if the living system demonstrates an adaptation process to changing environmental conditions. Different misinterpretations of the obtained results can, therefore, occur as a consequence of limitations of the standard statistical tools when it comes to analyzing nonstationary processes.

Aiming to illustrate how application of special tools of nonlinear and nonstationary time series analysis allows us to reveal new phenomena in the dynamics of living systems and to obtain more detailed information about the underlying biological processes, we presented three different wavelet analyses. In the first example, we considered sensory information processing in the rat trigeminal system. In order to study dynamical features in the functioning of neurons from different nuclei, we have proposed a new approach based on estimation of the stability of the firing response of a neuron to a repeating (oscillatory) stimulus. Using this approach, we have revealed clear distinctions in the dynamics of neurons from the Pr5 (principalis), Spi5 (interpolaris) and Spo5 (oralis) nuclei when stimulating the corresponding vibrissa by short air puffs. These neurons exhibit different behaviors under variation of the puff duration. While for Spo5 neurons the firing stability approaches a minimum for intermediate stimulus durations, Pr5 and Spi5—neurons demonstrate the presence of an 'optimum' stability as the stimulus duration is varied. We hypothesize that Pr5 and Spi5 process the tactile information in a similar way, paying attention mostly to the fast and precise identification of the stimulus presence, while Spo5 works on a longer time scale processing the fine structure of the stimulus. This new interpretation of the tactile information processing in the trigeminal complex of the rat requires further investigations and may significantly contribute to the existing knowledge about the information processing in the trigeminal sensory complex.

As the second example, we discussed intracellular interactions in snail neurons. Cell dynamics involves a number of regulatory processes that demonstrate different degrees of mutual interactions. The double-wavelet approach allowed us to reveal differences in modulation phenomena for the rhythms at 1 Hz and 2–4 Hz, thus providing information about the degree of interaction between different mechanisms in the cell functioning.

Interaction phenomena were also considered for the dynamics of nephron autoregulation. Using the depth of modulation as an informative characteristic of the mutual influence between the oscillatory modes, we have demonstrated the presence of essential distinctions in the functioning of nephrons from normotensive and spontaneously hypertensive rats. We have found that the processes of renal autoregulation in hypertensive rats involve a strong mode-to-mode interaction for all rhythmic components presented in the functioning of individual functional units of the kidney.

Key Point

- Various wavelet-based methods are proposed and applied to three different examples. The methods allow us to make a new interpretation of the tactile information processing in the trigeminal complex of the rat and to reveal essential distinctions in the response of neurons from different nuclei. The presence and features of nonlinear interactions among the neuronal processes in the form of frequency and amplitude modulation of fast processes by slower dynamics are revealed. Using the depth of modulation as an informative characteristic, essential distinctions in the mode-to-mode interactions for nephrons from normotensive and hypertensive rats are found.

Acknowledgments

We express our sincere thanks to F. Panetsos for providing experimental data for neurons from the trigeminal sensory complex and for fruitful discussions, to N.A. Brazhe, A.R. Brazhe, L.A. Erokhova and G.V. Maksimov for recordings of intracellular processes and many helpful discussions on cell dynamics, to N.-H. Holstein-Rathlou and D.J. Marsh for tubular pressure data and fruitful discussions of renal autoregulation mechanisms and to A.N. Tupitsyn for help with the data preprocessing. This work was partly supported by the European Union through the Network of Excellence BioSim, Contract No. LSHB-CT-2004-005137. A.N.P. acknowledges support from the Russian Ministry of Education and Sciences. V.A.M. acknowledges support from the Spanish Ministry of Education and Sciences under Ramon y Cajal program and a grant from Universidad Complutense (PR1/06-14482-B).

References

1. Hesch RD. *Endokrinologie* – Teil A, München: Urban and Schwarzenberg, 1989.
2. Glass L, Mackey MC. *From Clocks to Chaos: The Rhythms of Life*. Princeton: Princeton University Press, 1988.
3. Goldbeter A. (ed). *Cell to Cell Signalling: From Experiments to Theoretical Models*. London: Academic Press, 1989.
4. Gray CM, König P, Engel AK, *et al*. Oscillatory responses in cat visual cortex exhibit inter-columnar synchronization which reflects global stimulus properties. *Nature* 1989;**388**: 334–7.
5. Stern EA, Jaeger D, Wilson CJ. Membrane potential synchrony of simultaneously recorded striatal spiny neurons *in vivo*. *Nature* 1998;**394**:475–8.
6. Sosnovtseva OV, Pavlov AN, Brazhe NA, *et al*. Interference microscopy under double-wavelet analysis: a new tool to studying cell dynamics. *Phys Rev Let* 2005; **94**:218103.
7. Mosekilde E. *Topics in Nonlinear Dynamics: Applications to Physics, Biology and Economic Systems*. Singapore: World Scientific, 1996.
8. Grossman A, Morlet J. Decomposition of hardy functions into square integrable wavelets of constant shape. *SIAM J Math Anal* 1984;**15**:723–36.
9. Daubechies I. *Ten Lectures on Wavelets*. Philadelphia: SIAM, 1992.
10. Meyer Y. (ed). *Wavelets and Applications*. Berlin: Springer-Verlag, 1992.
11. Chui CK. *An Introduction to Wavelets*. New York: Academic Press, 1992.
12. Mallat SG. *A Wavelet Tour of Signal Processing*. San Diego: Academic Press, 1998.
13. Kantz H, Schreiber T. *Nonlinear Time Series Analysis*. Cambridge: Cambridge University Press, 2004.
14. Gabor D. Theory of communication. *J IEE* 1946;**93**: 429–57.
15. Peng C-K, Havlin S, Stanley HE, *et al*. Quantification of scaling exponents and crossover phenomena in nonstationary heartbeat time series. *Chaos* 1995;**5**:82–87.
16. Muzy JF, Bacry E, Arneodo A. The multifractal formalism revisited with wavelets. *Int J Bifurcation Chaos* 1994;**4**: 245–302.
17. Kaiser G. *A Friendly Guide to Wavelets*. Boston: Birkháuser, 1994.
18. Tuckwell HC. *Introduction to Theoretical Neurobiology*. Cambridge: Cambridge University Press, 1988, Vol. 1,2.
19. Arvidsson J. Somatotopic organization of vibrissae afferents in the trigeminal sensory nuclei of the rat studied by transganglionic transport of HRP. *J Comp Neurol* 2004;**211**: 84–92.
20. Darian-Smith I. The trigeminal system. In: Iggo A, (ed). *Handbook of Sensory Physiology*. Berlin: Springer-Verlag, 1973;271–315.
21. Jacquin MF, Renehan WE, Rhoades RW, *et al*. Morphology and topography of identified primary afferents in trigeminal subnuclei principalis and oralis. *J Neurophysiol* 1993;**70**:1911–36.
22. Moreno A, Garcia-Gonzalez V, Sanchez-Jimenez A, *et al*. Principalis, oralis and interpolaris responses to whisker movements provoked by air jets in rats. *Neuroreport* 2005;**16**: 1569–73.
23. Tychinskii VP. Coherent phase microscopy of intracellular processes. *Phys Uspekhi* 2001;**44**:683–96.
24. Straub VA, Benjamin PR. Extrinsic modulation and motor pattern generation in a feeding network: a cellular study. *J Neurosci* 2001;**21**:1767–78.
25. Adison PS, Watson JN. Secondary transform decoupling of shifted nonstationary signal modulation components: application to photoplethysmography. *Int J Wavelets Multi Inform Process* 2004;**2**:43–57.
26. Sosnovtseva OV, Pavlov AN, Mosekilde E, *et al*. Double-wavelet approach to study frequency and amplitude modulation in renal autoregulation. *Phys Rev E* 2004;**70**:031915.
27. Marsh DJ, Sosnovtseva OV, Pavlov AN, *et al*. Frequency encoding in renal blood flow regulation. *Am J Physiol Regul Integr Comp Physiol* 2005;**288**:R1160–7.
28. Sosnovtseva OV, Pavlov AN, Mosekilde E, *et al*. Double-wavelet approach to studying the modulation properties of nonstationary multimode dynamics. *Physiol Measur* 2005;**26**:351–62.
29. Brazhe NA, Brazhe AR, Pavlov AN, *et al*. Unraveling cell processes: Interference imaging weaved with data analysis. *J Biol Phys* 2006 (in press).
30. Lin MW, Wu AZ, Ting WH, *et al*. Changes in membrane cholesterol of pituitary tumor (GH3) cells regulate the activity of large-conductance Ca^{2+} –activated K^{+} channels. *Chin J Physiol* 2006;**49**:1–13.
31. O'Connell K, Martens JR, Tamkun MM. Localization of ion channels to lipid raft domains within the cardiovascular system. *Trends Cardiovas Med* 2004;**14**:37–42.
32. Szucs A, Molnar G, Rozsa K. Periodic and oscillatory firing patterns in identified nerve cells of *Lymnaea Stagnalis* L. *Acta Biol Hung* 1999;**50**:269–78.
33. Schutt A, Bullock TH, Basar E. Odor input generates 1.5 Hz and 3 Hz spectral peaks in the *Helix* pedal ganglion. *Brain Res* 2000;**879**:73–87.
34. Peixoto N, Ramirez FJ, Javier F. Helix aspersa identified neurons on multielectrode-array: Electrical stimulation and recording. Forum of Eur Neurosci Soc-FENS2000, Brighton, UK, 155.
35. Holstein-Rathlou N-H, Leyssac PP. TGF-mediated oscillations in the proximal intratubular pressure: differences between spontaneously hypertensive rats and Wistar-Kyoto rats. *Acta Physiol Scand* 1986;**126**:333–9.
36. Leyssac PP, Holstein-Rathlou N-H. Effects of various transport inhibitors on oscillating TGF pressure response in the rat. *Pflügers Arch* 1986;**407**:285–91.
37. Holstein-Rathlou N-H, Marsh DJ. Renal blood flow regulation and arterial pressure fluctuations: a case study in nonlinear dynamics. *Physiol Rev* 1994;**74**:637–81.
38. Sosnovtseva OV, Pavlov AN, Mosekilde E, *et al*. Bimodal oscillations in nephron autoregulation. *Phys Rev E* 2002;**66**:061909.
39. Holstein-Rathlou N-H, Yip K-P, Sosnovtseva OV, *et al*. Synchronization phenomena in nephron-nephron interaction. *Chaos* 2001;**11**:417–26.
40. Chon KH, Chen YM, Marmarelis VZ, *et al*. Detection of interactions between myogenic and TGF mechanisms using nonlinear analysis. *Am J Physiol Renal Physiol* 1994;**267**: F160–73.